Finite element analysis of the resurfaced femoral head

M Taylor
Bioengineering Sciences Research Group, School of Engineering Sciences, University of Southampton, Highfield, Southampton SO17 1BJ, UK. email: mtaylor@soton.ac.uk

The manuscript was received on 9 June 2005 and was accepted after revision for publication on 30 September 2005.

DOI: 10.1243/095441105X9363

Abstract: Failure of the resurfaced femoral head may occur in the short term owing to femoral neck fracture or in the long term owing to aseptic loosening as a result of strain shielding. Resurfacing arthroplasties are not all the same. In particular, there is considerable debate regarding the role of the metaphyseal stem and cementing technique. This study examines the influence of various metaphyseal stem configurations (diameter, percentage length in contact with bone, and bonded versus debonded) and cement mantle thickness on the load transfer within the femoral head. Resurfacing resulted in significant strain shielding in the superior femoral head and elevated strain in the superior femoral neck. Although the increase in strain in the femoral neck was significant, the mean strains were below the yield strain for cancellous bone. Peak strains were observed above the yield strain, but they accounted for less than 1 per cent of the total head–neck bone volume and therefore were unlikely to result in femoral neck fracture. Increasing the stem diameter and increasing the percentage stem length in contact with bone both increased the degree of strain shielding. Bonding the metaphyseal stem produced the most dramatic strain shielding, which also extended into the head–neck junction. In contrast, varying the cement mantle thickness had a negligible effect on the load transfer.

Keywords: resurfaced femoral head, finite element analysis

1 INTRODUCTION

Femoral head resurfacing has several advantages over conventional total hip arthroplasty which include minimal bone resection, easier revision, and maintenance of physiological stresses within the proximal femur. The short-term performance of modern hip resurfacing arthroplasty is impressive, with low rates of migration [**1**, **2**], revision [**3**, **4**], and femoral neck fracture [**5**]. There are two modes of failure for the resurfaced femoral head that are of concern: femoral neck fracture and aseptic loosening [**6**]. In the latest generation of resurfacing arthroplasty, femoral neck fracture rates are low and those that do occur have been attributed to varus orientation of the head or notching of the femoral neck [**5**]. Typically, fractures occur soon after the operation, usually within the first 15 weeks. In the longer term, failure of the supporting bone as a result of strain shielding inside the femoral head [**7**] may be a problem.

Although at first sight all designs of resurfacing femoral head look the same, there are subtle variations in design that may influence the load transfer within the femoral head. There are a number of factors likely to influence the loads, including the shell thickness, the internal geometry, the design of the metaphyseal stem, and how it contacts the bone and the cement mantle thickness. There is considerable debate regarding the role of the metaphyseal stem and there are, broadly speaking, two schools of thought. The first recommends that the metaphyseal stem should only be used as a locating device and, once implanted, should ideally play no part in load transfer [**8**]. Alternatively, Amstutz *et al.* [**4**] advocate cementing the metaphyseal stem in small femoral heads in order to maximize the available fixation area. However, there is concern that cementing the metaphyseal stem will increase the degree of strain shielding within the femoral head. The current generation of hip resurfacing relies on cement fixation of the femoral component. Two cementing techniques have emerged. The first technique utilizes low-viscosity cement [**9**] which provides greater penetration into the cancellous bone, generating cement mantles of 3–4 mm thick. The second tech-

nique uses higher-viscosity cement which produces a thinner cement mantle of around 1–1.5 mm [**6**]. In both cases, the design of the metaphyseal stem and the thickness of the cement mantle, there has only been limited analysis to see how they influence the load transfer in the resurfaced femoral head.

Finite element analysis has been used extensively to analyse the load transfer within the implanted proximal femur using conventional hip stems [**10**], but there have been relatively few studies examining the resurfaced femoral head [**7**, **11**, **12**]. Huiskes *et al.* [**12**] and de Waal Malefijt and Huiskes [**7**] used two-dimensional representations to model the resurfaced femoral head. Using an axisymmetric model of the head–neck region, Huiskes *et al.* [**12**] concluded that the Wagner prosthesis lead to stress protection within the femoral head and unnatural stresses at the bone–implant interface that may enhance interface failure and bone remodelling. In a study of the TARA prosthesis, de Waal Malefijt and Huiskes [**7**] examined the influence of stem length, using a two-dimensional side-plated model. They concluded that the cancellous bone within the femoral head is stress protected, particularly superiorly, and that a long, fully bonded stem accentuates the degree of stress shielding. Udofia *et al.* [**13**] examined the contact mechanics of metal-on-metal bearings used for resurfacing on the basis of axisymmetric and simplified three-dimensional models and commented that the degree of stress shielding was less than that seen in conventional joint replacement. Watanabe *et al.* [**11**] produced a three-dimensional finite element model of an epoxy composite femur with a McMinn prosthesis. They found stress shielding in the antero-superior region of the cancellous bone within the femoral neck, near the head–neck junction, and concluded that this may lead to femoral neck fractures in osteopenic patients. A significant limitation of all three studies was that, by assuming a single modulus, they did not account for the variation in material properties in the cancellous bone. Also, none of the studies performed analyses of the intact femur, to act as a reference for any quantitative comparison.

The aim of the present study was to analyse the resurfaced femoral head and, in particular, to examine the influence of the metaphyseal stem and cement mantle thickness on the load transfer compared with the intact femur.

2 METHODS

A solid model of a femur was generated from computed tomography (CT) scans (kindly provided by DePuy International, Leeds, UK) of a cadaveric femur from a donor weighing 77 kg. For each CT slice, the outer contour of the femur was defined as a polynomial spline (Mimics, Leuven). These curves were then lofted together (I-DEAS10 EDS, Texas) to form a three-dimensional solid model of the femur. The femur was then virtually implanted with a suitably sized femoral component (ASR, DePuy International, Leeds, UK). In the default implanted femur model, the prosthesis was considered as having a cemented inner surface, with a thickness of 3 mm superiorly and 1.5 mm around the parallel section (see Fig. 1). Although in reality the cement will be interdigitated with the cancellous bone, for simplicity this was modelled by a layer of cement only. The implant–cement and cement–bone interfaces were assumed to be rigidly bonded. A 6 mm (largest diameter) tapered metaphyseal stem was modelled as debonded and overreamed over its entire length. Contact was simulated between the metaphyseal stem and bone, in case the stem came into contact when loaded, and a coefficient of friction of 0.4 was assumed. All models were meshed using linear tetrahedral elements. A more refined mesh (1.5–1.6 mm average element edge length) was used in the head and neck regions, with larger elements (4–6.5 mm average element edge length) being used in the femoral shaft to reduce computational running costs. Material properties were applied to the bone using the freeware program BoneMat [**14**]. The Young's modulus of a bone element was calculated from the

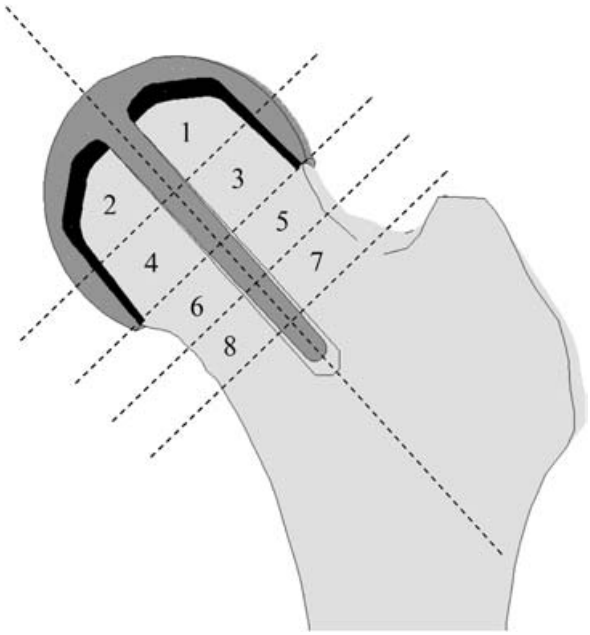

Fig. 1 Regions of interest defined within the implanted femur

average apparent density determined from CT scans and automatically assigned to the FE model using Bonemat. The apparent density was related to the Young's modulus by the equation [**15**]

$$E = 7821\rho^{1.53} \quad (1)$$

where E is the Young's modulus (MPa) and ρ is the apparent density (g/cm^3). The Poisson's ratio for bone was assumed to be 0.3. The resulting distribution of material properties in the intact femur are shown in Fig. 2. The prosthesis was modelled as having a Young's modulus of 200 GPa and a Poisson's ratio of 0.3. The polymethyl methacrylate (PMMA) bone cement was modelled as having a Young's modulus of 2.8 GPa and a Poisson's ratio of 0.3. The models were loaded with a 300 per cent body weight (BW) force applied to the femoral head and a 100 per cent BW force acting as the abductor muscles, both acting at 20° from the vertical in the frontal plane (Fig. 2). Both forces were distributed over an area to avoid the effects of point loading. For the intact femur, the joint reaction force was non-uniformly distributed over an approximately circular patch 3cm in diameter. The resulting area of 7 cm^2 is comparable with that reported by Brown and Shaw [**16**] within the intact femur to experience contact pressures greater than 1 MPa at similar load levels. The non-uniform distribution was arbitrarily simulated by applying uniform loads to three concentric rings of nodes such that 60 per cent of the resultant joint contact force was applied at radii between 0 and 0.75 cm, 30 per cent was applied between radii of 0.75 and 1.1 cm, and the remaining 10 per cent between radii of 1.1 and 1.5 cm. The models were rigidly constrained at the distal surface.

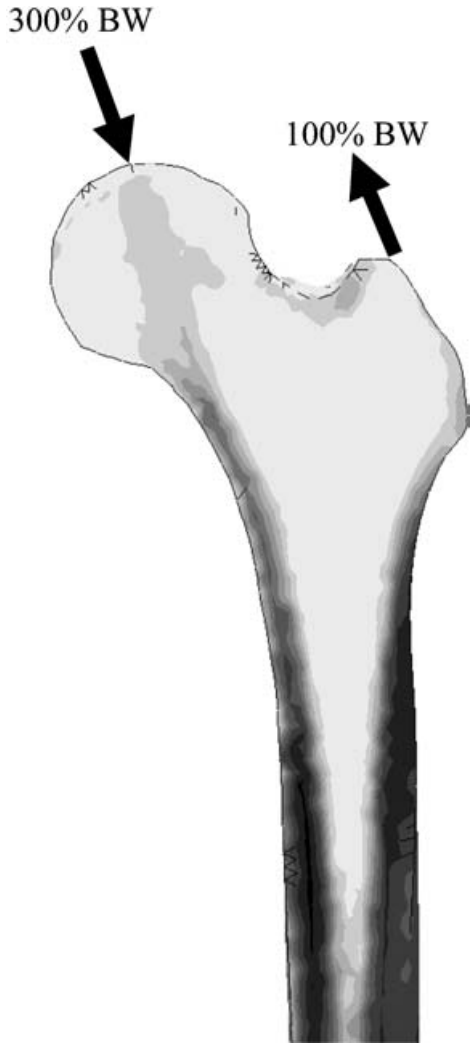

Fig. 2 Cross-section through the intact femur, illustrating the material property distribution and forces applied to the model of the intact femur (white corresponds to $E = 0$ GPa and black corresponds to $E > 12$ GPa)

Although it is more common to analyse load transfer in terms of stress, recent work has suggested that strain-based analysis may in fact be more relevant [**17**]. It has been found that the yield strain of trabecular bone is uniform within an anatomic site (i.e. it does not depend on the apparent density) [**18**] and is believed to be isotropic [**17**]. Based on this assumption, the effective strain has been used to assess the load transfer in the intact and implanted femoral head within this study

$$\varepsilon_{eq} = \frac{1}{\sqrt{2}}[(\varepsilon_1 - \varepsilon_2)^2 + (\varepsilon_2 - \varepsilon_3)^2 + (\varepsilon_3 - \varepsilon_1)^2]^{1/2} \quad (2)$$

In order to perform a quantitative comparative analysis, each model was divided into 16 regions of interest (ROI), eight anteriorly and eight posteriorly, as shown in Fig. 1. These regions of interest make it possible to determine the effect the implant has on the strain experienced in any particular bone volume with respect to the intact femur. The percentage change in strain was calculated as follows

$$\text{PD} = \left(\frac{\varepsilon_{\text{implanted}} - \varepsilon_{\text{intact}}}{\varepsilon_{\text{intact}}} \right) \times 100 \quad (3)$$

All analyses were run using the Marc 2001 software (MSC Software, Camberley, UK), and scripts were written automatically to calculate the mean and peak strain within each region of interest.

As discussed earlier, there are a number of issues related to implant design that may influence the load transfer in the resurfaced femoral head, and two aspects were investigated in detail: the role of the metaphyseal stem and the influence of the cement mantle thickness.

2.1 Investigation of the role of the metaphyseal stem

In the default model, the maximum pin diameter was 6 mm and had a 1.5° taper, and this was inserted into a parallel-sided hole, 6 mm in diameter, ensuring there was no contact along the length of the metaphyseal stem. The influence of the degree of contact between the pin and the bone was examined by starting the parallel-sided hole at a stem diameter corresponding to 0 (default), 50, and 100 per cent of the stem length. As discussed earlier, contact elements were used at the interface between the stem and bone. This process was repeated with a larger stem diameter of 9 mm. A further two analyses were performed in which the stem was assumed to be rigidly bonded to the surrounding bone over the entire length of the stem, simulating the cemented condition. This was done for both the 6 mm and the 9 mm stem diameters.

2.2 Influence of the cement mantle thickness

In addition to the default model, uniformly thick (3.5 mm) and thin (1.5 mm) cement mantles were analysed to represent the cement mantles generated using high- [**4**] and low-viscosity cement [**9**].

3 RESULTS

Usually, the stress distribution has been reported when analysing the load transfer in the proximal femur. For the sake of comparison, the von Mises stress distribution was examined [Fig. 3(a)] and found to be similar to that commonly reported in the literature, with the highest stresses being generated in the regions of highest-stiffness bone [Fig. 3(a)]. The load is transferred from the point of load application, through the dense cancellous bone in the femoral head to the cortical bone of the medial femur. The strain distribution [Fig. 3(b)] looks significantly different. There is a strain concentration immediately beneath the load application point, with further strain concentrations occurring inferiorly and superiorly at the head–neck junction. It is worthwhile noting that all regions of interest within the head, neck, and diaphyseal femur experience similar strain magnitudes. The predicted mean strain values within the head and neck are all within the range of 1300–2600 microstrains. The peak strain predicted in all the ROI was below 6000 microstrains. The volume of bone experiencing strain magnitudes greater than 5000 microstrains was less than 0.1 per cent of the total volume of interest. Therefore, the mean and peak strains were found to be lower than the 7000 microstrains yield limit reported for cancellous bone [**18**].

Insertion of the femoral component significantly alters the strain distribution within the femoral head and neck. As can be seen in Fig. 4(a), there was substantial strain shielding, particularly deep within the femoral head (ROI 1 and 2). Reductions of up to 59 per cent (Table 1) were predicted in the superior head region. There is an increase in the mean strains at the head–neck junction (ROI 3 and 4), with an increase of 11 per cent in the superior sections (ROI

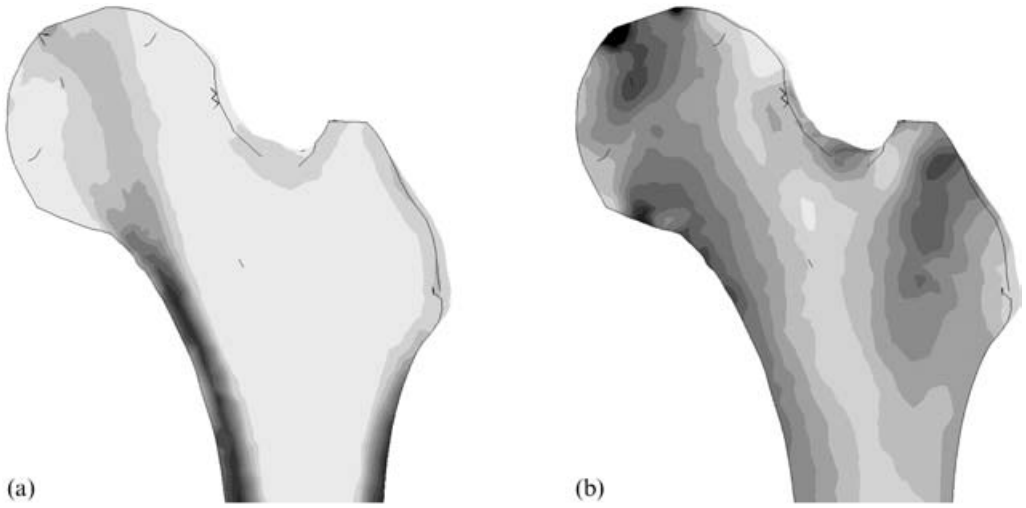

Fig. 3 Stress and strain distribution within the intact femur: (a) von Mises stress distribution (white corresponds to 0 MPa and black corresponds to stresses in excess of 25 MPa); (b) effective strain (white corresponds to 0 microstrain and black corresponds to in excess of 5000 microstrains)

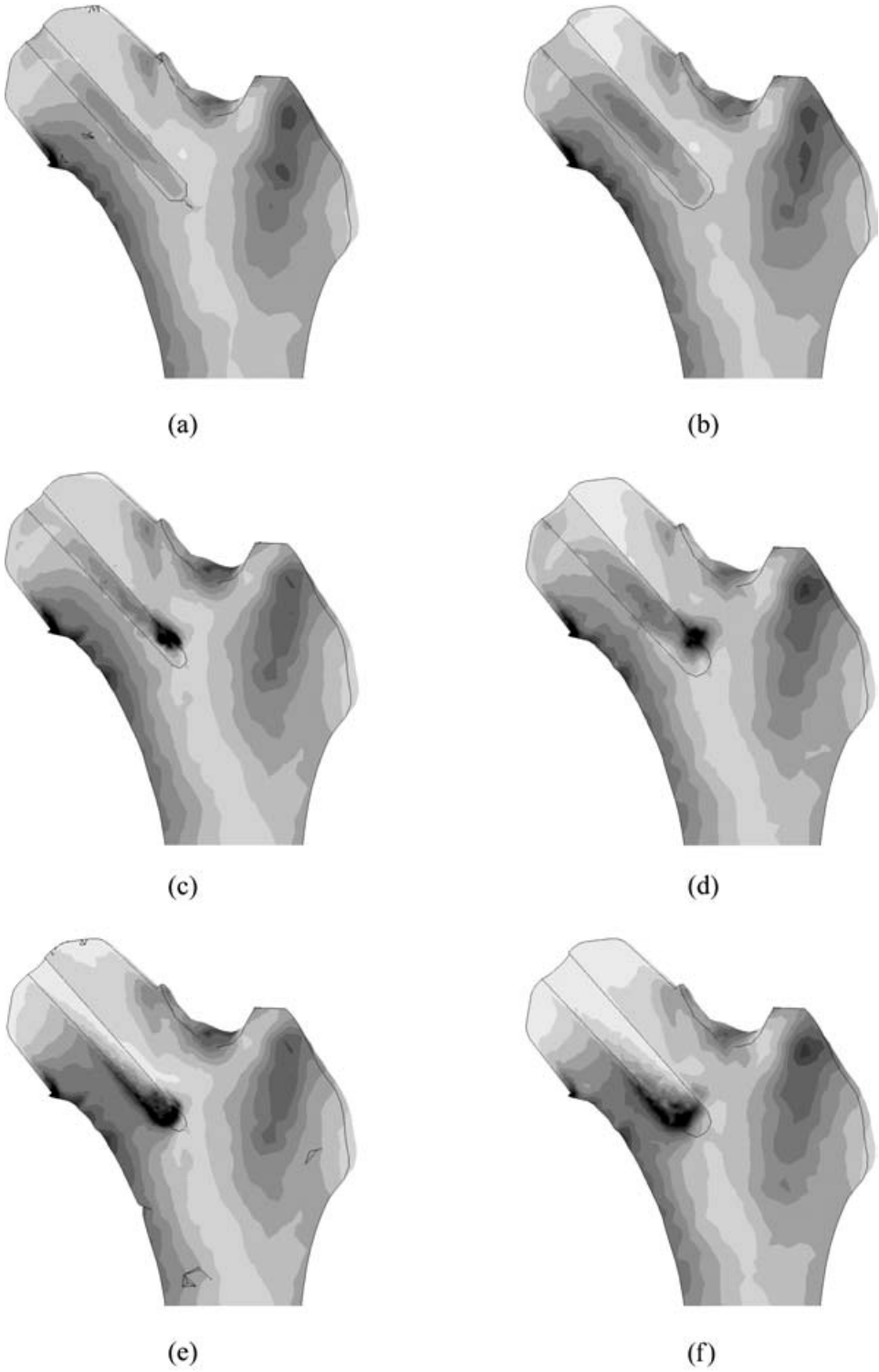

Fig. 4 Strain distribution within the resurfaced femoral head for various metaphyseal pin configurations (white corresponds to 0 microstrain and black corresponds to in excess of 5000 microstrains): (a) default model (6 mm stem, debonded, overreamed); (b) 9 mm stem, debonded, overreamed; (c) 6 mm stem, debonded, 100 per cent stem–bone contact; (d) 9 mm stem, debonded, 100 per cent stem–bone contact; (e) 6 mm stem, bonded; (f) 9 mm stem, bonded. Note that the prosthesis and cement mantle have been removed to aid visualization of the results

3). This increase in strain continues into the superior femoral neck (ROI 5 and 7), where there is an increase of up to 19 per cent in the predicted mean strain. Distal to the femoral neck, the strain distribution is similar to that of the intact femur. Peak strains of 13 700 microstrains were observed at the inferior head–neck junction (ROI 4). However, analysis of the strains exceeding 5000 microstrains only accounted for less than 1 per cent of the entire head-neck bone volume (approximately 30 000 mm^2).

In relation to the 6 mm diameter metaphyseal stem, increasing the length of the stem in contact with the bone did not significantly alter the strain distribution [Figs 4(a) and (c), Table 1]. There was a marginal increase in the superior femoral neck (ROI 5 and 7) where the mean strain, as compared with the intact femur, rose from 19 to 29 per cent. Also, in the case of the stem contacting over its entire length, there is a notable strain concentration at the distal tip. There was little or no difference in the strain distribution when the metaphyseal stem diameter was increased from 6 to 9 mm, assuming no contact over the entire stem length. However, as the length of the stem in contact increases, the strain magnitudes at the head–neck junction tend to decrease (ROI 3 and 4) and the strains in the superior femoral neck (ROI 5 and 7) tend to increase [Figs 4(b) and (d), Table 1]. There was also an increase in the strain concentration at the distal tip of the stem, as compared with the 6 mm diameter stem.

Bonding the stem to the surrounding bone produced the most significant changes in the strain distribution. For the 6 mm diameter stem [Fig. 4(e)], the degree of strain shielding inside the head (ROI 1 and 2) increased and there was a corresponding decrease in the strain magnitudes at the head–neck junction (ROI 3 and 4). The 9 mm diameter stem produced the greatest degree of strain shielding. There was a 79 per cent strain reduction in the superior sections (ROI 1 and 2) and also significant strain shielding at the head–neck junction (ROI 3 and 4), with a reduction of up to 38 per cent compared with the intact femur. Altering the cement mantle thickness from 1.5 to 3.5 mm did not produce any significant changes in the strain distribution within the resurfaced femoral head.

4 DISCUSSION AND CONCLUSIONS

As has been shown previously, resurfacing does alter the load transfer in the femoral head. When the stiff femoral component is inserted with a debonded, overreamed metaphyseal stem, the load is transferred around the periphery of the metallic component and exits at the head–neck junction. This results in the characteristic strain shielding of the superior femoral head and elevated strains at the head–neck junction. When the metaphyseal stem is cemented in place, load can also be transferred down the stem, increasing the strain shielding within the femoral head and resulting in a strain concentration at the distal tip of the stem.

From a purely mechanical perspective, there are

Table 1 Comparison of the predicted mean strain for each region of interest for the various metaphyseal stem configurations. Note that all implant configurations resulted in significant strain reductions in the superior femoral head (ROI 1 and 2) and increase in the strain in the superior femoral neck (ROI 5 and 7). Fully bonding a thick metaphyseal stem enhanced the degree of stress shielding

Region of interest (ROI)		Absolute mean strain in the intact femur (microstrains)	Percentage change in mean strain in implanted femur as compared with intact femur					
			Default model	Debonded, thick stem, 0% contact	Debonded, thin stem, 100% contact	Debonded, thick stem, 100% contact	Bonded thin stem	Bonded thick stem
1	Anterior	1988	−59	−66	−61	−65	−71	−78
	Posterior	1992	−59	−64	−62	−66	−72	−79
2	Anterior	2360	−55	−51	−56	−53	−71	−79
	Posterior	1970	−53	−48	−53	−50	−68	−77
3	Anterior	1390	9	12	8	−3	8	−29
	Posterior	1490	11	11	5	−3	1	−33
4	Anterior	2600	−1	9	3	−7	−1	−38
	Posterior	2600	−2	14	6	−7	3	−37
5	Anterior	1340	19	29	27	16	23	0
	Posterior	1270	18	26	22	18	28	−3
6	Anterior	2400	4	7	4	1	4	−13
	Posterior	2800	8	16	15	4	20	−7
7	Anterior	1340	12	18	26	20	16	6
	Posterior	1220	12	18	24	14	21	8
8	Anterior	2200	−2	−1	−1	0	6	8
	Posterior	2680	6	10	−4	−19	12	23

two possible modes of failure that are of concern in the resurfaced femoral head: in the short term femoral neck fracture and in the long term aseptic loosening as a consequence of strain shield induced bone resorption. All the variations in the resurfaced femoral head examined in this study predicted an increase in the mean strain observed in the superior femoral neck, as compared with those found in the intact femur. Although significant, the magnitude of the mean strains was still well below the yield strain for bone. Similar to the findings of Watanabe *et al.* [**11**], strain concentrations with magnitudes of up to 14 000 mirostrains were observed at the head–neck junction (Fig. 4). However, an analysis of the volume of bone exceeding the yield strain in the head–neck region never exceeded 1 per cent (approximately 300 mm^3) of the total bone volume (30 000 mm^3). Keyak and Rossi [**19**] compared the femoral neck fracture load predicted using linear elastic finite element models with that measured experimentally. In the FE models they used the criterion that 400 mm^3 of bone in the femoral neck should exceed the failure strain of bone, which was defined as 11 000 microstrains. They found a strong correlation between the measured fracture load, which ranged from 3 to 15 kN [**20**], and the predicted fracture load. However, the FE models consistently underpredicted the measured fracture load. In the present study, a more conservative failure strain has been adopted, of 7000 microstrains, and smaller volumes of failing bone have been observed. This would suggest that, for all of the configurations examined in this study, fracture of the femoral neck would be unlikely. The risk of femoral neck fracture in the current generation of femoral head resurfacing is low [**5**] and has been associated with notching of the femoral neck, improper seating of the femoral component, and excessive varus orientation of the component. In this study, the component was well aligned and fully seated and care was taken not to notch the neck. Further work is required to assess if these factors do increase the strains in the femoral neck, thus increasing the risk of femoral neck fracture.

Clinical migration studies [**1**, **2**] have shown that there is little or no migration of the femoral component within the first two post-operative years. Taylor and Tanner [**21**] hypothesized that migration is a result of the time-dependent failure of the supporting cancellous bone owing to overload. In general, the predicted strains within this study, for both the intact and implanted femur, are low. The mean strains are typically in the range of 1500–3000 microstrains as compared with the yield strain of cancellous bone of 7000 microstrains. For level gait, this would suggest that failure of the supporting cancellous bone, which would result in implant migration, is unlikely to occur.

Although early finite element studies have predicted that stress or strain shielding will occur within the femoral head, particularly superiorly [**7**, **12**], to date this does not appear to be affecting the short- to medium-term clinical results. However, with the resurgence of resurfacing arthroplasties and their implantation into younger, more active patients, this may well be a problem in the future. In line with previous finite element studies [**7**, **12**], significant strain shielding was observed within the femoral head. Unlike previous studies, it was possible to quantify the degree of strain shielding by direct comparison of the implanted femur results with those for the intact femur. For the default model (which consisted of a 6 mm diameter metaphyseal stem that did not contact the bone over its length), a reduction of up to 59 per cent in the mean strain was predicted within the femoral head. Increasing the metaphyseal stem diameter and increasing the length of the stem in contact with bone resulted in a small increase in the strain shielding in the superior femoral head (ROI 1 and 2). At the head–neck junction (ROI 3 and 4), the predicted strains were near physiological, with a marginal increase compared with the intact femur, for the majority of metaphyseal stem configurations examined. There was a significant increase in the mean strains found in the superior femoral neck (ROI 5 and 7), with strain increases of up to 29 per cent compared with the intact femur. In contrast, smaller deviations in the strain between the intact and implanted femur were predicted for the inferior femoral neck (ROI 6 and 8). The changes in strain in the femoral neck are in agreement with the bone density changes reported in clinical studies. As the femoral component covers the bone in the superior femoral head, no clinical data, in the form of DEXA studies, exist that examine the true extent of strain shielding that occurs *in vivo*. However, Kishida *et al.* [**22**] performed a DEXA study of the femoral neck of patients receiving a resurfaced femoral head and reported an increase of up to 11 per cent in the bone mineral density in the superior femoral neck in a 2 year period, but no significant changes in bone mineral density were observed in the inferior femoral neck.

The most significant changes in the load transfer occurred when the metaphyseal stem was bonded in place, simulating a cemented stem. The degree of strain shielding increased throughout the head (ROI 1 to 4). In particular, with the large-diameter pin, strain shielding extended to the head–neck junction (ROI 3 and 4). The strain magnitudes were also

reduced in the femoral neck. Although Amstutz *et al.* [**4**] recommend cementing the stem in small femoral heads in order to enhance fixation, the results of this study would suggest that doing so increases the degree of strain shielding. This may increase the risk of femoral neck thinning that has been observed in some patients [**8**].

The present study does have its limitations. Simulations have been performed on a single femur from a donor of average weight. The applied loads replicate the peak forces associated with the stance phase of level gait and were applied over a small area to minimize the effects of point loading. However, in the intact femur there was a strain concentration at the point of load application. In the comparative study, this may result in an overestimation of the strain shielding predicted in ROI 1 and 2 but is unlikely to affect the results within the other regions of interest. The femoral component was well aligned and a uniform-thickness cement mantle was modelled. The cement mantle has been modelled as a layer of pure bone cement. In reality, there will be a thin layer of bone cement and a composite layer of cement interdigitated with bone. Clinical studies have shown that the incidence of failure, for whatever reason, is low and, when failure does occur, it is associated with malorientation and poor surgical technique. In order adequately to assess the potential risk of failure, further work is required to study the extremes of loading and component placement. In spite of these limitations, this study has shown the following.

1. Significant strain shielding does occur in the superior femoral head, with strain reductions between 60 and 80 per cent compared with the intact femur.
2. The strains in the superior femoral neck are elevated in comparison with the intact femur, but are not likely to cause femoral neck fracture.
3. Cementing the metaphyseal stem increases the degree of strain shielding, particularly with a large-diameter metaphyseal stem.
4. Varying the cement mantle thickness does not significantly alter the load transfer in the resurfaced femoral head.

REFERENCES

1 **Itayem, R., Arndt, A., Nistor, L., McMinn, D.,** and **Lundberg, A.** Stability of the Birmingham hip resurfacing arthroplasty at two years. *J. Bone Jt Surg.*, 2005, **87B**, 158–162.

2 **Glyn-Jones, S., Gill, H. S., McLardy-Smith, P., and Murray, D. W.** Roentgen stereophotogrammetric analysis of the Birmingham hip resurfacing arthroplasty. *J. Bone Jt Surg.*, 2004, **86B**, 172–176.

3 **Treacy, R., McBryde, C. W.,** and **Pynsent, P. B.** Birmingham hip resurfacing arthroplasty: a minimum follow-up of five years. *J. Bone Jt Surg.*, 2005, **87B**, 67–170.

4 **Amstutz, H. C., Beaule, P. E., Dorey, F. J., Le Duff, M. J., Campbell, P. A.,** and **Gruen, T. A.** Metal-on-metal hybrid surface arthroplasty: two to six year follow-up study. *J. Bone Jt Surg.*, 2005, **86A**, 28–39.

5 **Shimmin, A.** and **Back, D.** Femoral neck fractures following Birmingham hip resurfacing. *J. Bone Jt Surg.*, 2005, **87B**, 463–464.

6 **Amstutz, H. C., Campbell, P. A.,** and **Le Duff, M. J.** Fracture of the neck of the femur after surface arthroplasty of the hip. *J. Bone Jt Surg.*, 2004, **86A**, 1874–1877.

7 **de Waal Malefijt, M. C.** and **Huiskes, R.** A clinical, radiographic and biomechanical study of the TARA hip prosthesis. *Arch. Orthop. Trauma Surg.*, 1993, **112**, 220–225.

8 **Back, D. L., Dalziel, R., Young, D.,** and **Shimmin, A.** Early results of primary Birmingham hip resurfacings. *J. Bone Jt Surg.*, 2005, **87B**, 324–329.

9 **McMinn, D., Treacy, R., Lin, K.,** and **Pynsent, P.** Metal on metal surface replacement of the hip – experience of the McMinn prosthesis. *Clin. Orthop. Rel. Res.*, 1996, **329**, S89–S98.

10 **Prendergast, P. J.** Finite element models in tissue mechanics and orthopaedic implant design. *Clin. Biomechanics*, 1997, **12**, 343–366.

11 **Watanabe, Y., Shiba, N., Matsuo, S., Higuchi, F., Tagawa, Y.,** and **Inoue, A.** Biomechanical study of the resurfacing hip arthroplasty. *J. Arthroplasty*, 2000, **15**, 505–511.

12 **Huiskes, R., Strens, P. H. G. E., Heck, V.,** and **Slooff, T. J.** Interface stresses in the resurfaced hip. *Acta Orthop. Scand.*, 1985, **56**, 474–478.

13 **Udofia, I. J., Yew, A.,** and **Jin, Z. M.** Contact mechanics analysis of metal-on-metal hip resurfacing prostheses. *Proc. Instn Mech. Engrs, Part H: J. Engineering in Medicine*, 2004, **218**, 293–305.

14 **Zannoni, C., Mantovani, R.,** and **Viceconti, M.** Material properties assignment to finite element models of bone structures: a new method. *Med. Engng Phys.*, 1998, **20**, 735–740.

15 **Destresse, B., Hobatho, M. C.,** and **Darmana, R.** Étude des propriétés mécaniques de l'os spongieux du tibia humain par une méthode ultrasonore. *Innov. Tech. Biol. Med.*, 1995, **16**, 288–299.

16 **Brown, T. D.** and **Shaw, D. T.** *In vitro* contact stress distributions in the natural human hip. *J. Biomechanics*, 1983, **16**, 373–384.

17 **Chang, W. C. W., Christensen, T. M., Pinilla, T. P.,** and **Keaveny, T. M.** Uniaxial yield strains for bovine trabecular bone are isotropic and asymmetric. *J. Orthop. Res.*, 1999, **17**, 582–585.

18 **Morgan, E. F.** and **Keaveny, T. M.** Dependence of yield strain of human trabecular bone on anatomic site. *J. Biomechanics*, 2001, **34**, 569–577.

19 **Keyak, J. H.** and **Rossi, S. A.** Prediction of femoral fracture load using finite element models: an examination of stress- and strain-based failure theories. *J. Biomechanics*, 2000, **33**, 209–214.
20 **Keyak, J. H., Rossi, S. A., Jones, K. A.,** and **Skinner, H. B.** Prediction of femoral fracture load using automated finite element modeling. *J. Biomechanics*, 1998, **31**, 125–133.
21 **Taylor, M.** and **Tanner, K. E.** Fatigue failure of cancellous bone: a possible cause of implant migration and loosening. *J. Bone Jt Surg.*, 1997, **79B**, 181–182.
22 **Kishida, Y., Sugano, N., Nishii, T., Miki, H., Yamaguchi, K.,** and **Yoshikawa, H.** Preservation of the bone mineral density of the femur after surface replacement of the hip. *J. Bone Jt Surg.*, 2004, **86B**, 185–189.